Electromagnetic Force Calculation of Conductor Plate Double Halbach Permanent Magnet Electrodynamic Suspension

Yin Chen and Kunlun Zhang

Key Laboratory of Magnetic Suspension Technology and Maglev Vehicle Ministry of Education
Chengdu Sichuan 610031, China
chenyin_swjtu@126.com, zhangkunlun@263.net

Abstract ─ In order to solve the problem of high drag force in traditional Permanent Magnet Electrodynamic Suspension (PM-EDS) and increase the levitation-drag force ratio, this paper proposes a new suspension system composed of conductor plates and a double Halbach permanent magnet array, and calculates its electromagnetic force. The eddy current distribution equation for the conductor plate and the analytic calculation formula for the electromagnetic force of the device are derived by solving the differential equations for the magnetic vector potential in space. Verifying the analytic method using the finite element method, the maximum and mean relative errors of the results were calculated to be 4% and 1.7%, respectively. This paper also compares the levitation-drag force ratio of the new suspension system with that of the traditional system and concludes that the new system can substantially reduce the drag force and power loss.

Index Terms ─ Analytic calculation, conductor plate, double Halbach array, electromagnetic field, Halbach permanent magnet electrodynamic suspension.

I. INTRODUCTION

The traditional PM-EDS structure is composed of conductor plates and a single Halbach permanent magnet array. One issue with this structure is its high electromagnetic drag force and power loss at the low speeds, making it unsuitable for urban rail transit. To overcome this disadvantage, the USA's GA developed a "null-current electrodynamic levitation system" composed of a Halbach array and independent coils [1-2]. This system can indeed reduce drag force considerably, but it is exceedingly complex and very difficult to manufacture. More importantly, its rail is composed of many independent coils, resulting in a discontinuous levitation force, which means an uncomfortable ride for passengers. In order to overcome these issues, this paper proposes the conductor plate double Halbach permanent magnet electrodynamic suspension.

Such suspension system consists of a non-magnetic conductor plate and two sets of Halbach arrays provided on the upper and lower sides of the conductor plate, respectively; when the upper and lower air gaps are unequal, the conductor plate will generate the induced current, thus, giving rise to levitation force. Its nature is the dynamic characteristics between the permanent magnet and metal plate, and when studying such electromagnetic device, it's often to employ the numerical computation [3-7]. Usually, the numerical computation results are accurate, but fail to reflect the inherent relations among different parameters. While studying such issues with the analytic method, due to the complexity of electromagnetic field calculations, the conductor plate is often supposed to be infinitely thick or thin, for the purpose of simplifying the study [8-9]. Yet, the current skin depth is a function of the speed, and hence, the speed range that can be studied using this method is rather limited. The literature [8] has, when studying the single Halbach permanent magnet electrodynamic suspension, regarded the conductor plate to be infinitely thin, and therefore, replace the volume current by surface current; however, this method only coincides

Submitted On: December 31, 2013
Accepted On: October 5, 2014

with the experimental results in a small medium speed range. Literature [10] takes into account the effect of conductor plate thickness, but the model boundary selected makes the equation too complex and the expression for the eddy current in the conductor plate cannot be derived from it. Another common analytic method is the equivalent circuit model; i.e., to create an equivalent circuit of the electromagnetic device and calculate the electromagnetic force based on the energy conversion theory [11-12]. Since the equivalent inductance of the plate-type device is difficult to solve, such method is only suitable for the suspension system consisting of coils and permanent magnets. What's more, permanent magnet linear motors have the similar electromagnetic property, but the permanent magnet motors are characterized by active control systems and constant secondary current, so its electromagnetic force calculation is simple, greatly different from the electromagnetic system studied in this paper [13-15].

Based on previous research, this paper proposes the conductor plate double Halbach PM-EDS scheme and investigates its electromagnetic property and electromagnetic force. The differential equation for magnetic vector potentials throughout the interior of the system is obtained and used to derive the magnetic field and eddy current distribution equation and the analytical expression for the electromagnetic force calculation. By verifying the analytic calculation result using the ANSYS and comparing the levitation-drag force ratio of the new suspension system with that of the traditional single Halbach PM-EDS, we conclude that the new system is indeed superior.

II. SUSPENSION MODLE

The cross section of the double Halbach suspension train, studied herein, is shown in Fig. 1.

The suspension system has a structure as shown in Fig. 2, where L is the thickness of non-magnetic conductor plate, τ, h and l are the polar distance, height of permanent magnet array and the thickness of the conductor plate, and d_1 and d_2 are the upper and lower air gaps.

If,

$$d_1 \neq d_2,$$

then, the air gap field

$$B_y \neq 0.$$

It will induce current in the metal plate and further give rise to electromagnetic force along the d_1=d_2 direction; thus, the system is able to achieve self-stabilized suspension. And as can be seen from the figure, as for the magnetic field generated in the air gap by the two sets of permanent magnet arrays, the Y components are offset, but X components are superimposed; hence, it can generate a greater levitation-drag force ratio than the single Halbach suspension [16].

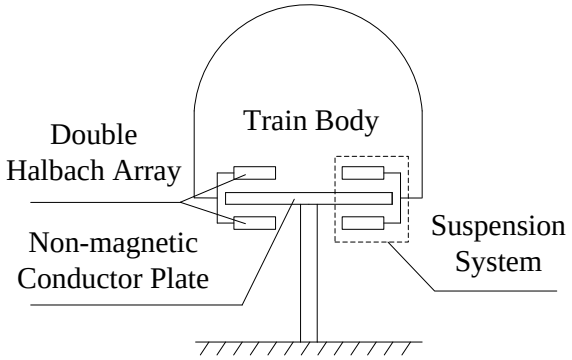

Fig. 1. Cross section of the conductor plate double Halbach PM-EDS train.

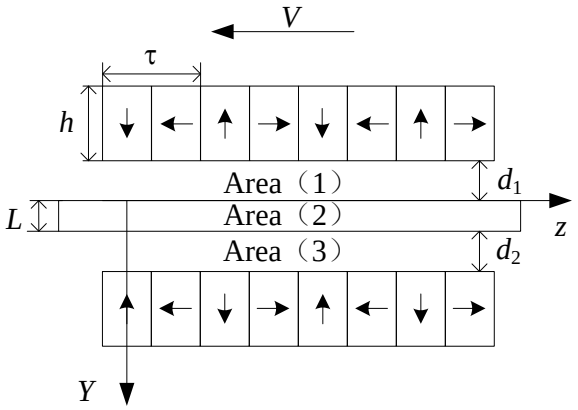

Fig. 2. Sketch diagram of conductor plate double Halbach PM-EDS train suspension system.

III. ELECTROMAGNETIC CALCULATION

A. Analytic calculation

The space magnetic field of permanent magnet Halbach array is expressed as [17]:

$$\begin{aligned} B_{y0} &= B_{m0} e^{j(pz+\omega t)} \\ B_{z0} &= B_{m0} e^{j(pz-\pi/2+\omega t)} \end{aligned}, \quad (1)$$

where, $p = \dfrac{\pi}{\tau}$, and

$$\begin{cases} B_{m0} = B_0 e^{-ps} \\ B_0 = B_r (1-e^{-ph}) \sin(\dfrac{\pi}{m}) / (\dfrac{\pi}{m}) \end{cases}. \quad (2)$$

Here, B_r is the remanence of permanent magnet, m means the number of modules contained in a pair of poles (Fig. 1 shows a 4-module structure, m=4), s stands for the distance from one point in the air gap to the lower surface of permanent magnet. The air gap field of double Halbach permanent magnet array may be expressed as:

$$\begin{cases} B_{sy} = B_0 (e^{-p(y+d_1)} - e^{-p(-y+d_2+l)}) e^{j(pz+\omega t)} \\ B_{sz} = B_0 (e^{-p(y+d_1)} + e^{-p(-y+d_2+l)}) e^{j(pz-\pi/2+\omega t)} \end{cases}, \quad (3)$$

where, B_0 may be determined by Equation (2), and for the convenience of expression, make:

$$\begin{cases} B_{ym} = B_0 (e^{-p(y+d_1)} - e^{-p(-y+d_2+l)}) \\ B_{zm} = B_0 (e^{-p(y+d_1)} + e^{-p(-y+d_2+l)}) \end{cases}. \quad (4)$$

When the conductor plate in Fig. 1 moves in the +Z direction at a relative speed of v, the surface density of eddy current generated in the conductor plate can be expressed as:

$$\begin{cases} \mathbf{J}_s = \gamma \mathbf{E}_s \\ \mathbf{E}_s = \mathbf{v} \times \mathbf{B} \end{cases}. \quad (5)$$

The Equation above may be shown as a scalar equation:

$$J_s = -\gamma v B_{sy}. \quad (6)$$

Based upon the Lorenz Gauge [18],

$$\nabla \mathbf{A} - \frac{k^2}{j\omega} \varphi = 0. \quad (7)$$

Obtain the magnetic vector potential equation,

$$\nabla^2 \mathbf{A} + k^2 \mathbf{A} = -\mu \mathbf{J}_s. \quad (8)$$

In the two-dimensional model, the magnetic vector potential **A** only has X component, and thus, for Areas (1)-(3) indicated in Fig. 1, the equation above may, based on the scalar equation, be expressed as:

$$\begin{cases} \nabla^2 A_{ix} + k_i^2 A_{ix} = 0 & (i = 1,3) \\ \nabla^2 A_{ix} + k_i^2 A_{ix} = -\mu_0 J_s & (i = 2) \end{cases}, \quad (9)$$

where, k_i is a propagation function [19],

$$k_i^2 = -j\omega\mu_0(\gamma_i + j\omega\varepsilon). \quad (10)$$

Here, γ_i is the conductivity of air ($i = 1,3$) and the conductor plate ($i = 2$). Formula (9) is partial differential equations, the solution to which requires the establishment of boundary condition equations [20] against different area joint faces.

(1) Infinity boundary condition:

$$\begin{cases} \lim\limits_{y \to -\infty} A_{1x} = 0 \\ \lim\limits_{y \to +\infty} A_{3x} = 0 \end{cases}. \quad (11)$$

(2) Inner boundary condition of joint face:

$$\begin{cases} A_{1x} = A_{2x} & (y = 0) \\ A_{2x} = A_{3x} & (y = L) \end{cases}. \quad (12)$$

(3) Tangential boundary condition of magnetic field:

$$\begin{cases} H_{1z} - H_{2z} = K_0 & (y = 0) \\ H_{2z} - H_{3z} = K_L & (y = L) \end{cases}, \quad (13)$$

where, K_0 and K_L are the linear current density at joint faces, and the surface current density in the conductor plate is J_e, then,

$$\begin{cases} K_0 = \int_{0^-}^{0^+} J_e \mathrm{d}y = 0 \\ K_L = \int_{L^-}^{L^+} J_e \mathrm{d}y = 0 \end{cases}. \quad (14)$$

And according to the relation between the magnetic field intensity and magnetic vector potential,

$$H_{iz} = -\frac{1}{\mu_0} \frac{\partial A_{ix}}{\partial y}. \quad (15)$$

Taking (14) and (15) into (13) may obtain:

$$\begin{cases} -\dfrac{\partial A_{1x}}{\partial y} - (-\dfrac{\partial A_{2x}}{\partial y}) = 0 & (y = 0) \\ -\dfrac{\partial A_{2x}}{\partial y} - (-\dfrac{\partial A_{3x}}{\partial y}) = 0 & (y = L) \end{cases}. \quad (16)$$

And the general solution of Formula (9) is [18]:

$$\begin{cases} A_{1x} = (C_1 e^{-R_1 y} + C_2 e^{R_1 y}) e^{(jpz+\omega t)} \\ A_{2x} = (C_3 e^{-R_2 y} + C_4 e^{R_2 y} + \theta(y)) e^{(jpz+\omega t)} \\ A_{3x} = (C_5 e^{-R_3 y} + C_6 e^{R_2 y}) e^{(jpz+\omega t)} \end{cases}, \quad (17)$$

where,

$$\begin{cases} R_i = \sqrt{p^2 - k_i^2} \\ \theta(y) = \dfrac{\mu_0 \gamma v B_{ym}(y)}{k_2^2} \end{cases} . \quad (18)$$

C_1-C_6 are undetermined constants, and it can, based upon the boundary conditional expressions (11), (12) and (16), be determined that the magnetic field in the plate is the superposition of static magnetic field and induced magnetic field generated by the permanent magnet. As a result, the electromagnetic field and eddy current in the space may be expressed as:

$$\begin{cases} B_y = B_{sy} + \dfrac{\partial A_{2x}}{\partial z} \\ B_z = B_{sz} + (-\dfrac{\partial A_{2x}}{\partial y}) \\ J_e = -\gamma v B_y = -\gamma v (B_{sy} + jpA_{2x}) \end{cases} . \quad (19)$$

Levitation force and drag force may be expressed as:

$$\begin{cases} F_y = -\dfrac{1}{2}\mathrm{Re}(\int_{2\tau}(\int_0^L J_e B_z^* dy)dz) \\ F_z = \dfrac{1}{2}\mathrm{Re}(\int_{2\tau}(\int_0^L J_e B_y^* dy)dz) \end{cases} , \quad (20)$$

where, B_y^* and B_z^* are the conjugate complex numbers of magnetic fields in *Y* and *Z* directions.

B. Finite element calculation

With ANSYS, this paper has established the conductor plate double Halbach PM-EDS finite element models. The model parameters are shown in Table 1 below.

Table 1: Model parameters

Parameters	Symbol	Values
Polar distance	τ	100 mm
Remanence	B_r	1.277 T
Height of magnet	h	50 mm
Thickness of plate	L	3 mm
Resistivity of plate	ρ	3.92e^{-8} Ωm
Upper air gap	$d1$	26 mm
Lower air gap	$d2$	32 mm
Width of model	L_x	100 mm

The element is PLANE53, and in view of the fact that materials in the model are of linear characteristics, it is hence to adopt the SOLVE linear solving method. The number of nodes generated totals 81573, and that of elements is up to 26962. The distribution of magnetic induction lines at 200 km/h is shown in Fig. 3.

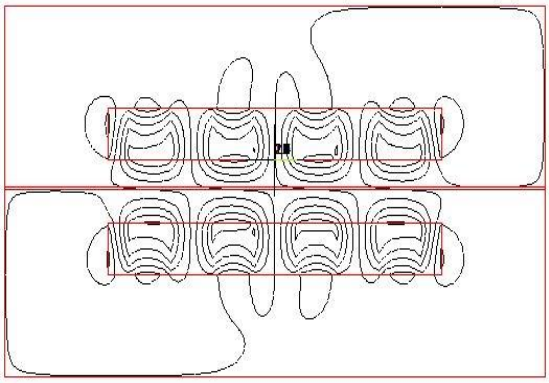

Fig. 3. Distribution of magnetic induction lines at 200 km/h.

To verify the validity of models, analytic and finite element methods are employed respectively to calculate the levitation force arising from the suspension system at 0-200 km/h under the parameters given in Table 1, as shown in Fig. 4.

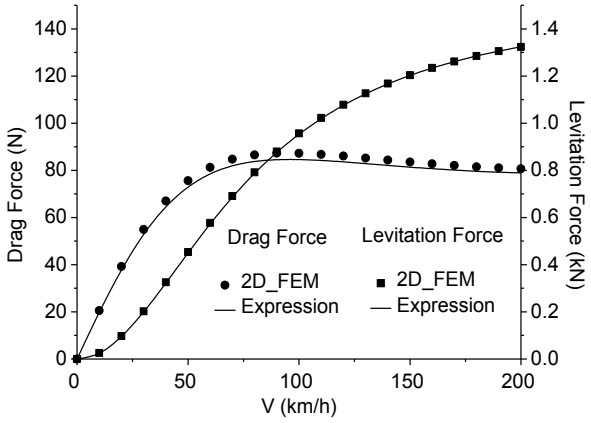

Fig. 4. Relations of electromagnetic force with the speed changes.

Figure 5 shows the relative errors between the analytic and finite element calculations at different speeds. It can be seen from the figure

that the maximum relative error is 4%, with a mean relative error of 1.7% only. Moreover, the maximum levitation error is just 1.2%.

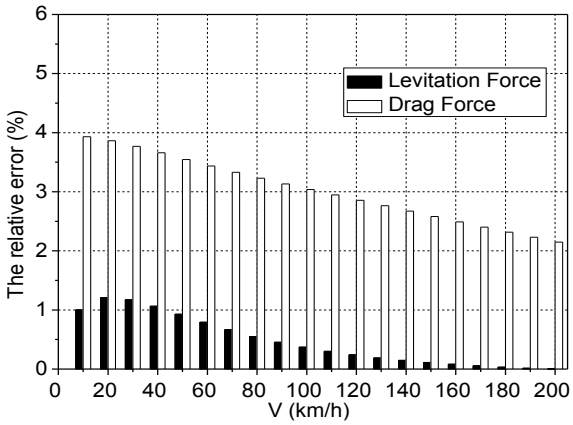

Fig. 5. Relative errors between the analytic and finite element methods.

IV. COMPARISON WITH THE TRADITIONAL SINGLE HALBACK PM-EDS

This paper proposes the conductor plate double Halbach PM-EDS scheme in order to increase the levitation-drag force ratio. To demonstrate its effectiveness, levitation-drag force ratio of both systems was calculated at different speeds. The parameters are shown in Table 2 and the structures of the single/double Halbach suspension systems are shown in Figs. 2 and 6 [10]. The single Halbach system has no permanent magnet array below it, so d_2 is ignored. All other parameters are the same.

Table 2: Parameters of the single/double Halbach systems

Parameters	Symbol	Values
Polar distance	τ	800 mm
Remanence	B_r	1.277 T
Height of magnet	h	300 mm
Thickness of plate	L	10 mm
Resistivity of plate	ρ	$3.92e^{-8}$ Ωm
Upper air gap	d_1	15 mm
Lower air gap	d_2	60 mm

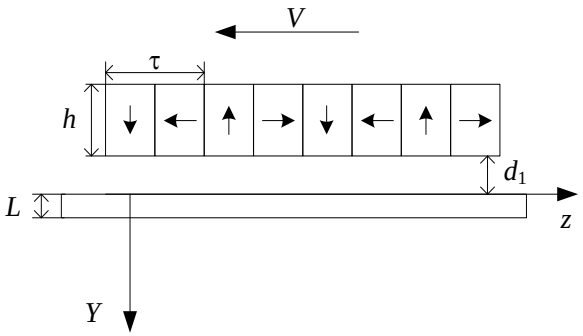

Fig. 6. Sketch diagram of conductor plate single Halbach suspension system.

The curve in Fig. 7 shows how the levitation-drag force ratio of the single and double Halbach suspension systems changes with speed. The figure indicates that, compared with the traditional single Halbach system, the double Halbach system considerably increases the levitation-drag force ratio. In applied engineering, when a maglev train is in a suspension state, the levitation force is equal to the gravity, which is a constant. Therefore, a greater levitation-drag force ratio means a smaller drag force and less power loss. This demonstrates the superiority of this new suspension system.

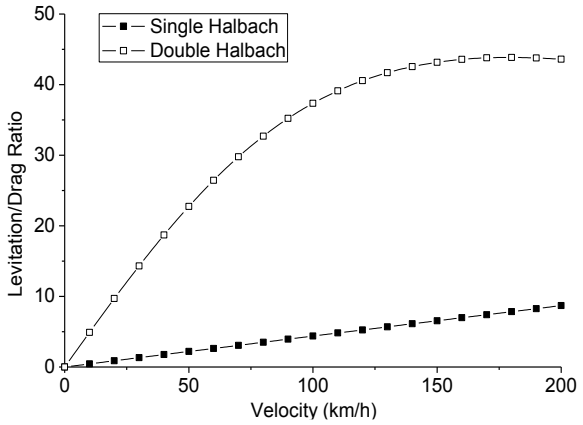

Fig. 7. Comparison of levitation-drag force ratios of single and double Halbach PM-EDS systems.

If η_1 and η_2 represent the levitation-drag force ratios of the single and double Halbach PM-

EDS systems, η_1/η_2 changes with speed as shown in the curve in Fig. 8.

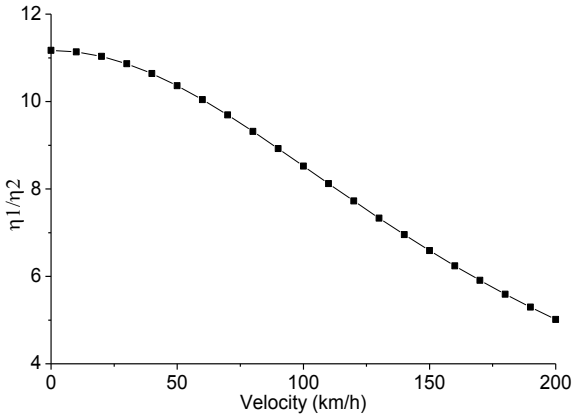

Fig. 8. Improvement of levitation-drag force ratio.

At different speeds, the double Halbach suspension system can increase the levitation-drag force ratio 5 to 11 times. Since the levitation-drag force ratio improvement decreases as speed increases, this improvement is more significant at low speeds. Therefore, the double Halbach system is more suitable for low-speed urban rail transit.

V. CONCLUSION

Based on the reference to relevant studies, this paper proposes the conductor plate double Halbach permanent magnet electrodynamic suspension to address issues with the existing system, provides the analytic calculation method applicable to this suspension model and proves the accuracy of this analytic method using the finite element method. Finally, this paper compares the levitation-drag force ratios of the two suspension systems to demonstrate that the double Halbach system can solve the problem of low levitation-drag force ratio and high drag force in the single Halbach system, and therefore, has positive significance for further research into electrodynamic suspension.

ACKNOWLEDGMENT

This material is based upon work supported by the Fundamental Research Funds for the Central Universities (2682013ZT18) and Doctor Innovation Funds of SWJTU (2014).

REFERENCES

[1] R. Kratz and R. F. Post, "A null current electrodynamic levitation system," *IEEE Transactions on Applied Superconductivity*, vol. 12, no. 1, pp. 930-932, 2002.

[2] Y. Wu, L. Yan, and S. Xu, "Inductrack technology and its application in maglev transport," *Electric Application*, vol. 25, no. 1, pp. 1-3, 2006.

[3] S. M. Jang, S. H. Lee, and S. S. Jeong, "Characteristics analysis of eddy-current brake system using the linear halbach array," *IEEE Transactions on Magnetics*, vol. 38, no. 8, pp. 2994-2996, 2002.

[4] S. M. Jang, S. S. Jeong, and S. D. Cha, "The application of linear halbach array to eddy current rail brake system," *IEEE Transactions on Magnetics*, vol. 37, no. 7, pp. 2627-2629, 2001.

[5] Z. Tan and Y. Li, "Development of flywheel energy storage system control platform based on dual-DSP," *Power System Protection and Control*, vol. 40, no. 11, pp. 127-139, 2012.

[6] P. Tang, Y. Qi, G. Huang, and T. Li, "Eddy current loss analysis of iron-less flywheel electric machine's winding," *Transactions of China Electrotechnical Society*, vol. 25, no. 3, pp. 27-32, 2010.

[7] Y. Huang, B. Fang, and J. Sun, "Simulation research on the microgrid with flywheel energy storage system," *Power System Protection and Control*, vol. 39, no. 9, pp. 83-113, 2011.

[8] C. Li, Y. Du, P. Xia, and L. Yan, "Analysis and experimental testing of EDS maglev with linear halbach and conducting sheet," *Transactions of China Electrotechnical Society*, vol. 24, no. 1, pp. 18-22, 2009.

[9] J. Wang, Y. Li, and L. Yan, "Study on applying the linear halbach array to eddy current brake system for maglev," *Electric Drive*, vol. 40, no. 5, pp. 8-11, 2010.

[10] H. W. Cho, H. S. Han, J. S. Bang, H. K. Sung, and B. H. Kim. "Characteristic analysis of electro dynamic suspension device with permanent magnet halbach array," *Journal of Applied Physics*, vol. 105, no. 7, pp. 3141-3143, 2009.

[11] R. F. Post and D. D. Ryutov, "The inductrack: a simpler approach to magnetic levitation," *IEEE Transctions on Applied Superconductivity*, vol. 10, no. 1, pp. 901-904, 2000.

[12] M. Toshiaki and H. Hitoshi, "Electromagnetic analysis of inductrack magnetic levitation," *Electrical Engineering in Japan*, vol. 142, no. 1, pp. 67-74, 2003.

[13] X. Huang, Q. Zhang, and G. Zhou, "Halbach permanent magnet iron-less linear motors," *Transactions of China Electrotechnical Society*, vol. 25, no. 6, pp. 1-6, 2010.

[14] P. Meng, X. Qiu, and W. Lin, "Study of the dynamic characteristics of directly driven permanent magnet synchronous wind turbine," *Power System Protection and Control*, vol. 40, no. 14, pp. 38-43, 2012.

[15] J. Fan, J. Wu, C. Li, et al., "Solution of permanent magnet synchronous motors with partition between poles halbach magnet," *Transactions of China Electrotechnical Society*, vol. 28, no. 3, pp. 36-42, 2013.

[16] Y. Zhang, D. Qiao, and J. Gao, "Current research on and applications of halbach permanent magnet array," *Analytical Instrumentation*, vol. 1, no. 2, pp. 5-10, 2010.

[17] J. F. Hoburg, "Modeling maglev passenger compartment static magnetic field from linear halbach permanent magnet arrays," *IEEE Transactions on Magnetics*, vol. 40, no. 1, pp. 59-64, 2004.

[18] Y. Chena and K. Zhang, "Calculation and analysis of the forces created by halbach permanent magnet electrodynamic suspension," *Applied Mechanics and Materials*, vol. 229, pp. 440-443, 2012.

[19] Y. Lei, "Analytic calculation of harmonic electromagnetic field," Beijing, China, 2000.

[20] C. Feng and X. Ma, "Introduction of engineering electromagnetic field," Beijing, China, 2000.